

Cellulose triacetate(CTA)-based forward osmosis membranes for water purification: optimization of dope solution composition and preparation conditions

Huaqiang Chu^a, Wenwen Zhang^a, Lin Wang^{b,c}, Xi Wei^a, Zhenjiang Yu^a, Yalei Zhang^a, Xuefei Zhou^{a,*}

^aState Key Laboratory of Pollution Control and Resource Reuse, School of Environmental Science and Engineering, Tongji University, Shanghai 200092, China, email: chuhuaqiang@tongji.edu.cn (H. Chu), zhangwenwen198@163.com (W. Zhang), 565006339@qq.com (X. Wei), yuzhenjiang_nju@126.com (Z. Yu), zhangyalei@tongji.edu.cn (Y. Zhang), Tel. +86-21-65985811, Fax +86-21-65985811, email: zhouxuefei@tongji.edu.cn (X. Zhou)

^bSchool of Municipal and Environmental Engineering, Shandong Jianzhu University, Jinan 250101, China, email: lynn04@126.com (L. Wang)

^cShandong Co-Innovation Center of Green Building, Jinan 250101, China

Received 21 July 2016; Accepted 11 January 2018

ABSTRACT

In this study, different PET support fabric based forward osmosis (FO) membranes were prepared and the optimal casting compositions as well as preparation conditions were investigated. The results showed that the optimal membrane casting solution compositions were 10.9% wt. CTA, 79.6% wt. solvents (the ratio of 1,4-dioxane and acetone is 6), (1,4-dioxane/acetone = 6/1), and 9.5% wt. additives (2.0% wt. PVP and 7.5% wt. lactic acid). In addition, the active layer formation was largely dependent on the thickness and pore size of PET support and the membrane on an 80- μm -thick PET support fabric with a pore size of 80 μm presented the best performance. Evaporation time, environmental humidity, annealing temperature and annealing time also played important roles on the membrane flux and reverse salt flux control. Experimental results found that high environmental humidity and a relatively low annealing temperature of 45°C was optimal for this work. The optimized membrane showed lower salt leakage than commercial HTI membrane. This lab-scale FO membrane with high salt rejection ratio and low back diffusion rate could provide a great option for a method of desalination and the detail influence of different casting compositions as well as preparation conditions on membrane performance present significant impacts on the industrial production of FO membrane.

Keywords: Forward osmosis; PET support fabric; Casting compositions; Preparation conditions; Antifouling performance

1. Introduction

Forward osmosis (FO), driven by the osmotic pressure difference across a semi-permeable membrane, has been one of the unique and emerging technologies that can produce both clean energy and water [1]. Compared to traditional pressure-driven membrane processes, FO offers recognized advantages including high rejections

to contaminants [2], low membrane fouling [3] and potentially less operation energy [4–5]. And it has been planned to be utilized in seawater and brackish desalination [4,6,7], wastewater treatment [8–11], power generation [12,13], food and pharmaceutical dehydration [14,15], etc. However, most of these applications are only in the experimental stage, as a result of the lack of appropriately designed and good performance commercial FO membranes in the current market.

*Corresponding author.

An ideal FO membrane should contain basic characteristics of high water flux, high salt rejection and low internal concentration polarization (ICP) [16]. Currently, the most widely commercially available FO membrane is fabricated by Hydration Technology Innovations (HTI, Albany, OR), which is an asymmetric flat sheet membrane made of cellulose triacetate (CTA) based solution, embedded with a polyester mesh via the phase-inversion method [17]. HTI FO membrane exhibits excellent performance with respect to high water flux and reasonable reverse salt flux; however, it is still limited due to problems related to severe ICP [1]. Herein, it is necessary to carry out new exploration and developments in phase inversion and membrane formation processes and consider their potential practical applications.

Phase inversion method has been widely used in membrane preparation. The polymer for the casting solution rapidly precipitates into surrounding non-solvent in the coagulation bath, forming a top layer on the membrane with a thin and compact structure and a porous layer under the top layer; thus, the basic structure of the membrane is obtained. Cellulose acetate (CA) polymers with different degrees of acetylation have long served as a model for the study of phase inversion mechanism and have been a popular material for various separation applications [18–22]. Due to the hydrophilic properties of CA polymers, membranes prepared by these polymers resist fouling relatively better than the conventional polyamide used in the FO process and thus favor a high water flux [23]. Another important advantage of CA polymers is that they are noted for their relatively low cost and environmentally friendly properties. In addition, support fabric provides mechanical support for membrane fabrication; meanwhile, its properties (porosity, thickness, pore size, etc.) have a great influence on phase-inversion-method membrane. Researchers found that the high porosity support layer exhibited higher water flux than the low porosity support layer, although they considered that the porosity had little effect on J_s (reverse salt flux), which was determined by the tightness of the dense layers [22]. Cellulose triacetate (CTA), as a type of CA polymer, also presented unique advantage in the process of FO membrane formation. However, to our best knowledge, few researches about the detail influences of casting compositions as well as preparation conditions on the membrane performance.

In this work, CTA is used as polymeric material for flat-sheet membrane preparation via the phase inversion method. Dual additive system-including polyvinylpyrrolidone (PVP) as an organic additive and lactic acid as a non-solvent additive—is introduced into the dope solution to enhance membrane performance. The effects of the CTA content, the solvent content ratio (1,4-dioxane/acetone) and the additive content on the membrane performance were investigated to confirm the optimized dope solution. Meanwhile, the effects of PET fabric (non-woven) properties of thickness and pore size on membrane performance are also studied. This work also reports the effects of preparation conditions, including evaporation temperature, evaporation time, environmental humidity, annealing temperature and annealing time, on water flux and reverse salt flux in the FO process.

2. Materials and methods

2.1. Materials and chemicals

Cellulose triacetate (CTA, 43–49% wt. acetyl) was purchased from Beijing Inno Chem Science & Technology Co., Ltd. 1,4-Dioxane, acetone, lactic acid and polyvinylpyrrolidone (PVP) were purchased from Sinopharm Chemical Reagent Company. Sodium chloride (NaCl, powder, $\geq 99.5\%$) was used as the solute of the draw solution. Five different types of polyester (PET) fabric, which were labeled P1–P5, were used as support layers for membrane formation, whose major differences were thickness, pore size and porosity.

2.2. Membrane preparation

The FO membrane utilized in this experiment was prepared via the immersion precipitation phase inversion process. Membrane casting solution was prepared by dissolving CTA (8.9–13% wt.) in 1,4-dioxane and acetone, with lactic acid and PVP as the pore-forming agents. The solution was vigorously stirred in a sealed three-necked flask for 24 h at room temperature ($20 \pm 3^\circ\text{C}$). After homogeneously mixing, the solution was sealed and remained static for 12–24 h for de-aeration. PET fabric was attached to a flat and clean glass plate using sticky tape. The solution was spread on the fabric with a casting knife that was set at the gate height of 180 μm . The nascent membrane was evaporated in the air for a certain time, followed by immediate immersion with the glass plate into deionized (DI) water for phase separation. After 2 h, the membrane was immersed in water with a different temperature and time for the annealing treatment, and then it was stored in DI water for further measurement.

2.3. Membrane performance testing

The FO membrane was fixed in a transparent organic glass cell that contained two symmetric channels with an effective area of 33.6 cm^2 (the cell is track type, the long is 11.5 cm and the width is 2.5 cm, elliptical diameter is 2.5 cm). The FS and DS were introduced and recirculated respectively by variable-speed gear pumps at the same speed. The FS tank was placed on a hotplate for stirring, and the conductivity of the FS was measured by a conductivity meter (Leici- DDSJ-308F, Shanghai Instrument Electric Science Instrument Co. Ltd.) for concentration conversion. The DS tank was placed on a balance (UX6200H, SHIMADZU (China) Co. Ltd.) connected to a computer to automatically record any weight changes. To eliminate gravitational effects, the FS tank and DS tank should remain at the same height. All the experiments were conducted at room temperature, and the FO membranes were tested in FO mode (active layers faced the feed solution).

Water flux (J_w , $\text{L}\cdot\text{m}^{-2}\cdot\text{h}^{-1}$, abbreviated as LMH) and reverse salt flux (J_s , $\text{mol}\cdot\text{m}^{-2}\cdot\text{h}^{-1}$) are basic indicators to evaluate membrane performance. In this work, DI water was used as the FS, and 2 MNaCl was used as the DS for the 1 h measurement. Water that permeated through the FO membrane from the FS to the DS was calculated by the change

in the weight of the DS. The amount of salt that diffused from DS to FS was determined by the conductivity change in the FS.

$$J_w = \frac{\Delta \text{weight}}{\text{water density} \times \text{effective membrane area} \times \Delta \text{time}} (\text{LMH}) \quad (1)$$

$$J_s = \frac{\Delta \text{mol of NaCl}}{\text{effective membrane area} \times \Delta \text{time}} (\text{mol} \cdot \text{m}^{-2} \cdot \text{h}^{-1}) \quad (2)$$

Both the weight change of the DS and the conductivity change of the FS were measured and stored on a computer at 60s intervals.

The membrane structural parameter S was calculated based on Eqs. (3) and (4) [24–25].

$$J_w = \frac{1}{K} \ln \left(\frac{B + A\pi_1}{B + J_w + A\pi_2} \right) \quad (3)$$

$$S = K \cdot D_s \quad (4)$$

where A is the water permeability coefficient of the membrane active layer, B is the salt permeability coefficient of the membrane active layer, K is the resistance to solute diffusion in the membrane support layer, D_s is the effective solute diffusion coefficient in the membrane support layer, π_1 is the osmotic pressure of the bulk draw solution, and π_2 is the osmotic pressure of the feed solution.

2.4. Analytical tools

2.4.1. Scanning electron microscopy (SEM)

Top surfaces and cross-section morphologies of the membrane were observed using a SEM (Philips XL 30, Netherlands). Small pieces of membrane samples were freeze-dried in a vacuum freeze dryer for 24 h. The dried membrane samples were fractured by liquid nitrogen and carefully mounted on a specimen with conductive tapes. Samples were coated with a layer of gold using a sputter coater (SCD 005) before SEM observation.

2.4.2. Viscosity measurements

The viscosity of the dope solution was measured using a digital viscosimeter (NDJ-8S, Shanghai Fangrui Equipment Co., Ltd., China) at 20°C, and the SP 4 spindle was used

with 6 revolutions per minute. Three measurements were taken, and the results were averaged for each substance.

2.4.3. Solubility parameter of mixed solvent (δ_{mix})

The solubility parameter is an important criterion for measuring the miscibility of the hybrid system.

$$\delta_{mix} = \delta_1 x_1 + \delta_2 x_2 \quad (5)$$

where x_1 and x_2 are molar volume concentration of component 1 and 2, and δ_1 and δ_2 are the solubility parameter of component 1 and 2.

2.4.4. Porosity

The support fabric porosity (%) is defined as a ratio of the total pore area to the analyzed area of the material. The analyzed image is observed by top-surface SEM.

The gravimetric method was utilized to obtain the membrane porosity by measuring the dry-wet weight of the membrane. Before measuring the wet weight of the membrane (m_1 , g), excess water should be quickly removed once the membrane is removed from the water bath. Then, the wet membrane is freeze dried overnight for re-weighing (m_2 , g). Thus the water content of the membrane can be calculated as $m_1 - m_2$, and the overall porosity, P (%), of the membrane is obtained using the following equation:

$$P = \frac{m_1 - m_2}{\rho_w \cdot a \cdot \varepsilon} \times 100 \quad (6)$$

where ρ_w (0.998 g/cm³) is the water density, a is the effective area (cm²), and ε is the thickness of the wet membrane (cm).

3. Results and discussion

3.1. Effects of polymer and solvents

The miscibility of polymer and solvents in a membrane solution system significantly affects membrane properties.

Polymer content influences the formation of the active layer and the pore structure of the FO membrane. In the solvent system used in this work, both solvents could form hydrogen bond with CTA, because they had similar hydrogen-bonding solubility parameters, as shown in Table 1.

Table 1
Physicochemical properties of polymer and solvents

Compounds	Density (g/mL)	Molecular weight (g/mol)	Vapor pressure/mm Hg (20°C)	Components of Solubility parameter (Mpa) ^{1/2}			Solubility parameter (Mpa) ^{1/2} δ
				Dispersive δ _D	Polar δ _P	Hydrogen-bonding δ _H	
CTA	–	–	–	15.55	–	10.64	18.84
1,4-Dioxane	1.03	88.11	27	19.0	1.8	7.4	20.5
Acetone	0.792	58.08	184	15.5	10.4	7.0	20.1

1,4-Dioxane is more favored for CTA than acetone because its ring system was more compatible with the pyranose rings of CTA [22]. The good hybrid compatibility of the solution resulted in a strong reaction between the solvents and the polymer. As a result, the polymer chains separated and greatly extended in the good solvent system.

As shown in Fig. 1, the CTA content that was less than 8.9% wt. was dilute to the extent that pin holes were easily generated to formed effective membrane. Contrarily, the solution with high CTA content (13% wt. in this study) easily brought air bubbles into the support layer, and the resulting casting membrane was defective and in homogeneous. J_w and J_s decreased when the CTA content increased from 8.9% wt. to 13% wt. When the CTA polymers are in high concentration, the polymer chains are in a high density and can be easier to aggregate for the possible roll of the polymer chains. As a result, the pore size of active layer decreased, and a dense layer formed. Meanwhile, when the nascent membrane was immersed in the coagulation bath, the high polymer concentration led to advanced gelation in the polymer/solvent/non-solvent ternary phase, promoting precipitation while hindering solidification, which helped to form a dense skin layer [26,27]. The relatively dense top layer then further hindered inter-diffusion between the solvent (outflow) and the non-solvent (inflow), which delayed solidification and led to the formation of a dense skin layer with a small pore size. Comprehensively considering the properties of the membranes, 10.9 wt.% CTA polymer was chosen as the optimal polymer content.

The evaporation rates of the solvents during the cast and outflow to the coagulation bath were known to be significant factors in the formation of the membrane top structure. Solvents that had good volatility and were favorably compatible with the polymer helped to form a dense active layer as the polymer concentration of the membrane top surface increased with the evaporation and outflow of the volatile solvents. It was obvious shown that J_w and J_s increased when the 1,4-dioxane/acetone ratio increased from 4 to 8 in Fig. 3. This is the result of a decrease in the total volatility of solvent mixture that occurred due to an increased 1,4-dioxane/acetone ratio. As shown in Table 1, 1,4-Dioxane and acetone

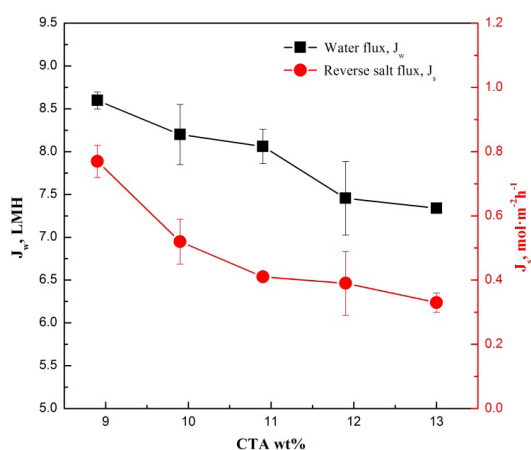


Fig. 1. Performance of FO membranes with different CTA weight concentration contents (% wt.), and 1,4-dioxane/acetone weight concentration ratios - 7/1, lactic acid - 7.5% wt., PVP - 1.9% wt.

have similar solubility parameters but different vapor pressures. The vapor pressure of acetone (184 mm Hg (20°C)) is much higher than that of 1,4-dioxane (27 mm Hg (20°C)), which indicated that acetone is more volatile than 1,4-dioxane. Less solvent evaporating from the casting film resulted in more porous top structures and obtained a relatively high water flux. Meanwhile, an increase in the 1,4-dioxane portion led to a more soluble solvent system for CTA, as the mixture solvent solubility parameter (δ_{mix}) decreased (Fig. 2) and became closer to the solubility parameter of CTA (Table 1). The slow outflow of solvents and the relatively fast inflow of surrounding water occurred simultaneously during phase inversion, which delayed de-mixing and resulted in a porous structure [28]. Solvents whose ratio of 1,4-dioxane/acetone was less than 4 could not completely dissolve the total CTA polymer content of 10.9% wt. Comprehensively, the optimal ratio of 1,4-dioxane/acetone is 6.

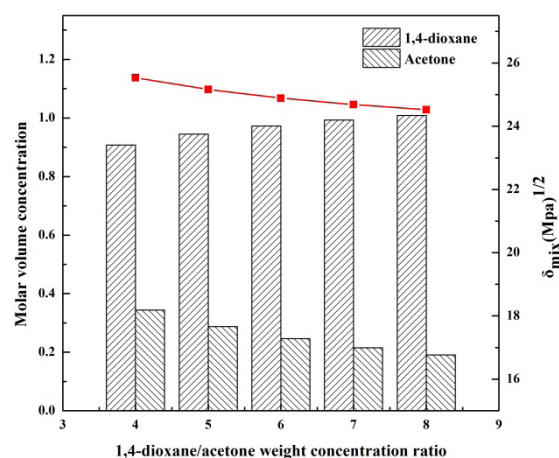


Fig. 2. Molar volume concentration of 1,4-dioxane and acetone and the solubility parameter of the mixture solvent (δ_{mix}) with a 1,4-dioxane/acetone weight concentration ratio of 4 to 8.

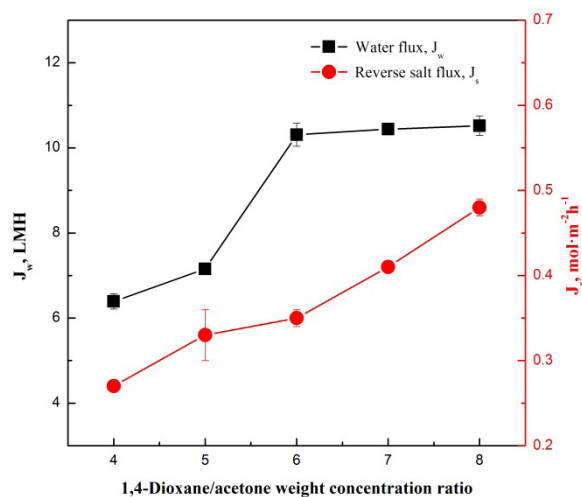


Fig. 3. Performance of FO membranes with different 1,4-dioxane/acetone weight concentration ratios, CTA - 10.9% wt., lactic acid - 7.5% wt., PVP - 1.9% wt.

Table 2
Effects of PVP on membrane performance

Membrane	Composition (% wt.)					Water flux	Reverse salt flux J_s (mol·m ⁻² ·h ⁻¹)
	CTA	1,4-Dioxane	Acetone	PVP	Lactic acid	J_w (LMH)	
1	10.9	69.1	11.5	1	7.5	8.63 ± 0.16	0.31 ± 0.05
2	10.9	68.3	11.3	2	7.5	10.31 ± 0.21	0.35 ± 0.12
3	10.9	67.4	11.2	3	7.5	7.55 ± 0.19	0.45 ± 0.14
4	10.9	66.5	11.1	4	7.5	7.06 ± 0.15	0.36 ± 0.17
5	10.9	65.7	10.9	5	7.5	6.79 ± 0.23	0.34 ± 0.11

Table 3
Viscosity of dope solution with respect to the lactic acid/PVP ratio

Membrane*	Additive composition (%wt.)		Viscosity (Pa·S)
	Lactic acid	PVP	
1#	8.4	1.1	33.3
2#	7.6	1.9	41.9
3#	6.3	3.2	52.2
4#	5.7	3.8	60.8
5#	4.8	4.7	69.2

*FO membranes were prepared with 10.9%wt CTA polymers, 79.6% wt. solvents (1,4-dioxane/acetone = 6/1), 9.5% wt. additives.

3.2. Effects of additives

In this study, PVP and lactic acid were used as pore-forming agents, which played different roles on the properties of the dope solution and membrane structure. As shown in Table 2, J_w and J_s exhibited similarly changing trends that first increased and then decreased slightly, as the PVP content increased from 1% to 5%. Increasing the PVP content may result in more porous supporting layers and the addition of finger-like pores in this layer, thus decreasing transfer resistance. However, PVP is a type of non-solvent swelling agent for the dope solution. When it is in high concentration, it could decrease the proportion of the solvent and solvent as an important pore-forming agent in the phase inversion process. There should be a balance point between PVP and the solvent. Meanwhile, a high PVP concentration simultaneously decreased the mutual diffusivities among the dope solution components and increased the viscosity of the solution. Herein, the membrane with 2% presented the best performance.

Lactic acid was a type of diluent for dope solution, which could be demonstrated by the viscosity of the casting solution that increased with the increasing lactic acid content of the mixture additive (Table 3). The solution with lower viscosity formed a more porous layer structure when immersed in the water bath.

In conclusion, the overall membrane casting solution that was composed of 10.9% wt. CTA, 79.6% wt. solvents (68.3% wt. 1,4-dioxane and 11.3% wt. acetone, 1,4-dioxane/acetone = 6/1), and 9.5% wt. additives (2.0% wt. PVP and 7.5% wt. lactic acid) was considered optimal for the procurement of membranes that perform well (Fig. 4).

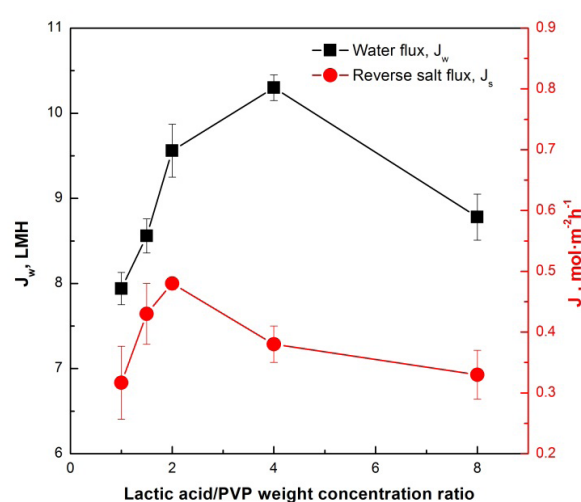


Fig. 4. Performance of FO membranes with different lactic acid/PVP weight concentration ratios, CTA-10.9% wt., solvents (1,4-dioxane/acetone = 6/1) - 79.6% wt., additives - 9.5% wt.

3.3. Effects of support fabric

It is commonly accepted that FO membrane performance is strongly dependent on both the active layer and support layer characteristics [29]. Until now, numerous efforts have been made to fabricate high performance thin film composite (TFC) FO membranes by preparing satisfying support layer structures [17,29,30]. Although the main role of the support layers used in the phase inversion method is the mechanical support on membrane formation, it still revealed great influence on the membrane performance. Thus, the optimal solution was to cast on five PET support fabrics (P1-5) with different thicknesses and pore sizes to assess their effects on membrane structure and performance.

As for the cross-sectional morphologies, both membranes showed asymmetrical structures consisting of selective layers on the top and bottom sides, embedded polyester (PET) fabric for support and a sublayer between the top surface and the support fabric. Indeed, the existence of the support fabric might alter the regular structure of sublayer to some degree. The membrane sublayers were softer when the solution coating on the support fabrics with larger pores. One reason might be that the dope solution more easily penetrated and aggregated in larger pores, resulting in a decrease of solution in the sublayer. Inversely, the PET fabrics with smaller pores present relatively poor permeation

of casting solution, led to a double layer or even a multilayer sublayer structure, as shown in Fig. 5(e') and (d'). In other words, the PET fabrics with smaller pore size can increase the resistance to water and solute molecule transmission. The support layer characteristics are listed in Table 4.

As shown in Table 4 and Fig. 6, membranes marked with M3, M4, and M5, which had smaller porosity support fabric, showed a poorer J_w than that of membrane M2. In fact, there exists a trade-off between the support layer properties (thickness and pore size) and the membrane performance.

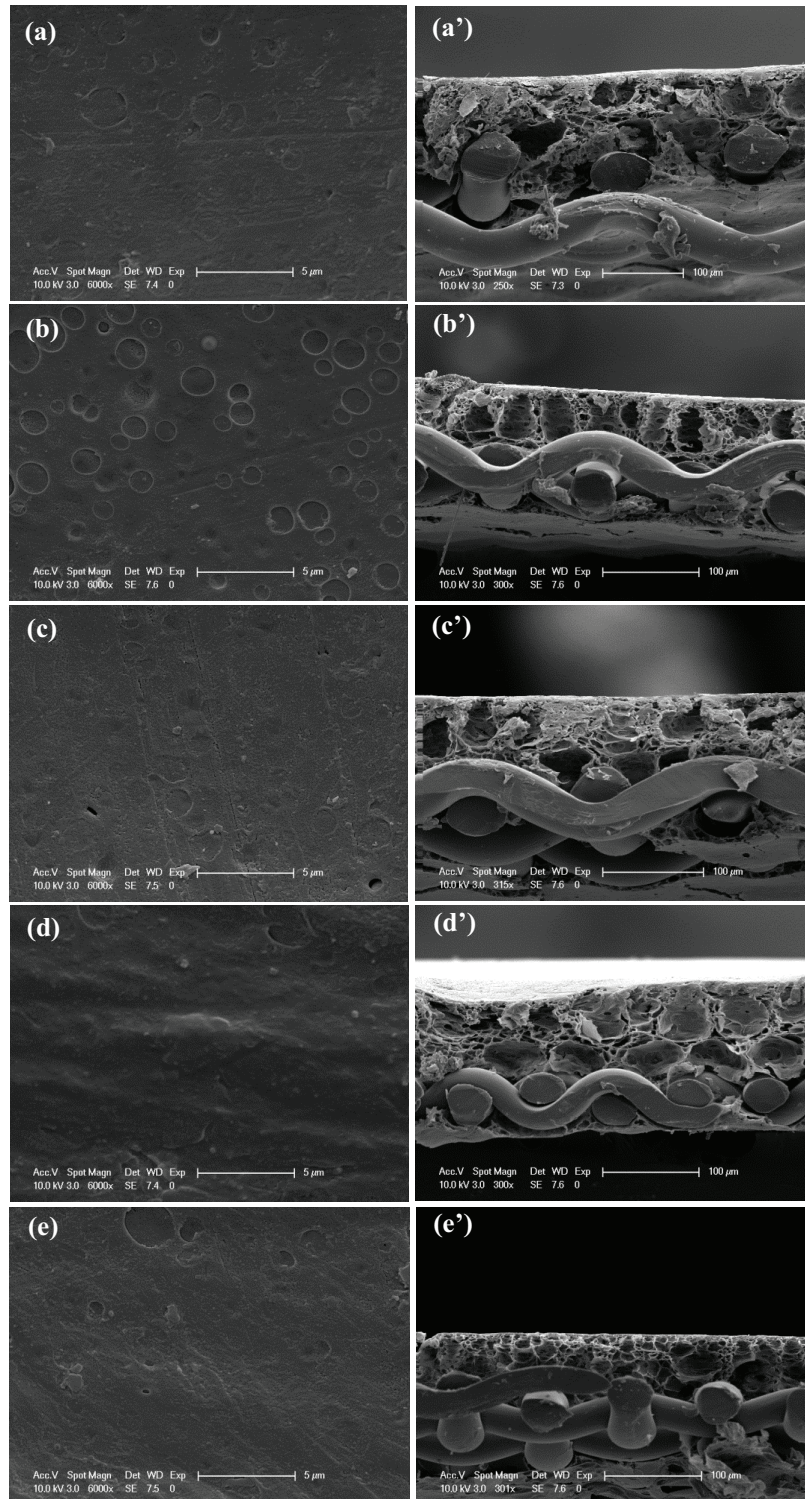


Fig. 5. Surface and cross-sectional SEM images of FO membranes with different support fabrics: (a) M1, (b) M2, (c) M3, (d) M4, (e) M5, (a') M1, (b') M2, (c') M3, (d') M4, (e') M5.

Table 4
Characteristics of support fabrics and membrane without and with support layers

	No. 1		No. 2		No. 3		No. 4		No. 5	
	P1	M1	P2	M2	P3	M3	P4	M4	P5	M5
Thickness (μm)	100	180	80	130	69	130	58	130	64	130
Porosity (%)	41	64.2	41	65.5	36	64.6	30	72.1	23	79.5
Pore size ^a (μm)	100	–	80	–	60	–	42	–	32	–

^aThe average pore size of support fabric.

P1-5 referred to support fabrics with different thickness and pore sizes.

M1-5 referred to FO membranes prepared by optimized dope solution casting on PET support fabric with different thickness and pore sizes.

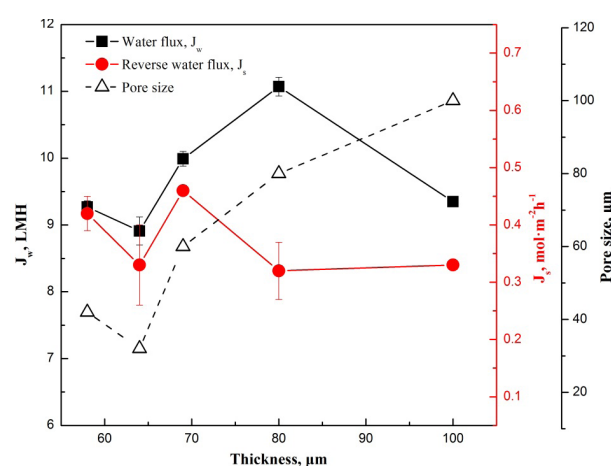


Fig. 6. Performance of membranes with PET fabrics with different thicknesses and pore sizes, CTA - 10.9% wt., solvents - 79.7% wt. (1,4-dioxane/acetone = 6/1), lactic acid - 7.5% wt., PVP - 1.9% wt.

Table 5
Effects of evaporation time on membrane performance

Membrane	Evaporation time (s)	Annealing temp ($^{\circ}\text{C}$)	J_w (LMH)	J_s ($\text{mol}\cdot\text{m}^{-2}\cdot\text{h}^{-1}$)
6	0	60	11.71 ± 0.21	0.51 ± 0.11
7	30	60	10.31 ± 0.18	0.31 ± 0.07
8	60	60	9.64 ± 0.25	0.29 ± 0.13
9	90	60	8.60 ± 0.11	0.23 ± 0.05

The detail balances can be described into three aspects: (a) the membrane performance changed along with the trend of the pore size when the support fabric thickness was below 70 μm , implying that the pore size significantly influenced the membrane properties when the support fabric was thin; the sublayer structure was tighter with increasing pore sizes; (b) the thickness and pore size had a combined influence on the membrane performance when both of them had moderate values (thickness of 69–80 μm , pore size of 36–41 μm); and (c) J_w decreased dramatically, while J_s changed mildly, when the thickness exceeded 80 μm and the pore size increased, which may have occurred because the relatively over large pore size had little effect on the dense layer formation that would determine salt rejection, resulting in the invariability of J_s ; mean-

while, the increasing thickness of the support layer brought resistance to water transmission, and as a result, J_w decreased. Considering that the thick support layer led to severe ICP problems and decreased water flux, along with support fabrics with large pores that could easily cause defective membranes, the desired fabric material used for membrane support layer should have a small thickness and an adequate pore size. High surface porosity at the support layer interface of the TFC membrane may improve the osmotic water flux [17]. To summarize, the membrane revealed the best performance by casting the dope solution on a 80- μm -thick PET support fabric with a pore size of 80 μm .

3.4. Effects of membrane preparation conditions

Evaporation time (the time gap between the membrane casting and the phase inversion) has a strong effect on the formation of the membrane structure, particularly the top surface (active layer), which imparts separation characteristics to the membrane [31]. The appropriate evaporation time offered enough time for solvent evaporation, resulting in an increase in polymer concentration on the top surface of membrane, and thus, the formation of a more compact active layer.

As shown in Table 5, both J_w and J_s decreased with the increase in evaporation time. Comprehensively considering the balance of J_w and J_s , the optimal evaporation time was confirmed as 30 s, and the membrane presented a high J_w of 10.31 ± 0.18 LMH and a reasonable J_s of 0.31 ± 0.07 $\text{mol}\cdot\text{m}^{-2}\cdot\text{h}^{-1}$ under this condition. As we know, acetone can be evaporated in the air, and then leads to the denser surface layer. But compared with the inter-diffusion between solvents and water molecules, the inter-diffusion is not very drastic in the air. Herein, the evaporation time should control in a reasonable range.

Environmental humidity can also have a great influence of membrane performance. Fig. 7 clearly reveals that the values J_w presented an obvious increase along with the humidity, while the J_s presented a reverse trend with that of J_w . The hydrophilic CTA polymer would tend to aggregate at the liquid-air interface on the top surface to form an active layer with a small pore size under a high humidity environment. Simultaneously, the loss of solvents through evaporation was reduced in higher humidity conditions. However, it would consume much energy to reach to the higher humidity. Therefore, there might be a balance point between the membrane performance and the energy consumption and 70% humidity was chosen as the optimal condition in this study.

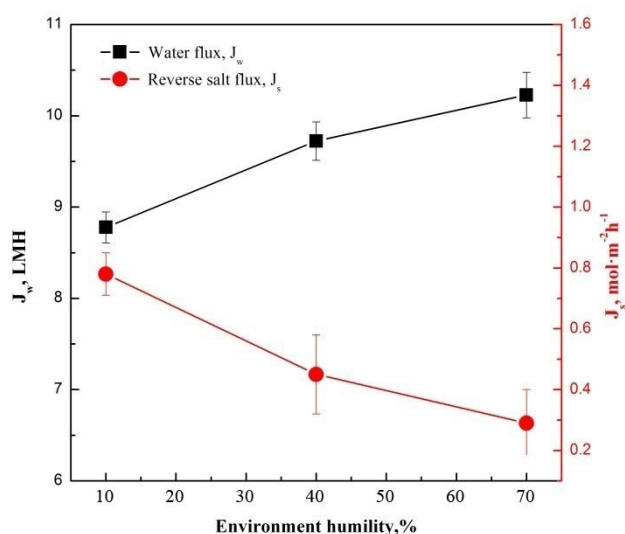


Fig. 7. Effects of environmental humidity on FO membrane performance.

Annealing treatment can help to convert the side chains of the cellulose acetate molecules from intra molecular to intermolecular hydrogen bonds, resulting in a reduction in the membrane pore size [32]. In this study, J_s decreased when the annealing temperature increased from 30 to 90°C, while J_w first increased from 30°C to 45°C and then decreased from 45°C to 90°C. The membrane performed best at an annealing temperature of 45°C (Fig. 8a). At annealing temperatures between 30–45°C, residual chemicals that were trapped in the membrane pores were released, resulting in a large pore size of the top surface. The residual solvents and additives were completely released when the membrane was annealed at 45°C, resulting in the highest J_w and a reasonable J_s . Simultaneously, low thermal energy provided by low annealing temperatures slightly shrank the membrane pores. The combined action of released chemicals and pore shrinkage changed the membrane pore size such that they were large enough to allow water to pass through while rejecting salt molecules. High annealing temperatures offered no beneficial effects for removing chemicals [22]. The relatively high thermal energy provided by the high annealing temperature had a significant effect on the formation of membrane properties, and hydrogen bonding between the polymer chains was enhanced, which led to smaller membrane pore sizes and more compact skin layers. As a result, J_w and J_s decreased as the annealing temperature increased from 45°C to 90°C, respectively.

Membranes not receiving annealing treatment exhibited poor salt-rejection performances, as shown in Fig. 8b. The J_s of the annealed membrane was increased by 157% when compared with the membrane that was annealed at 45°C for 10 min. However, when the membrane was annealed for 50 min, poor salt rejection occurred, which was similar to the annealed membrane. Membranes performed differently when annealing time increased from 10–30 min; the J_w decreased, and J_s increased when membranes were annealed at 45°C. Solvents and additives embedded within the membrane gradually washed out as

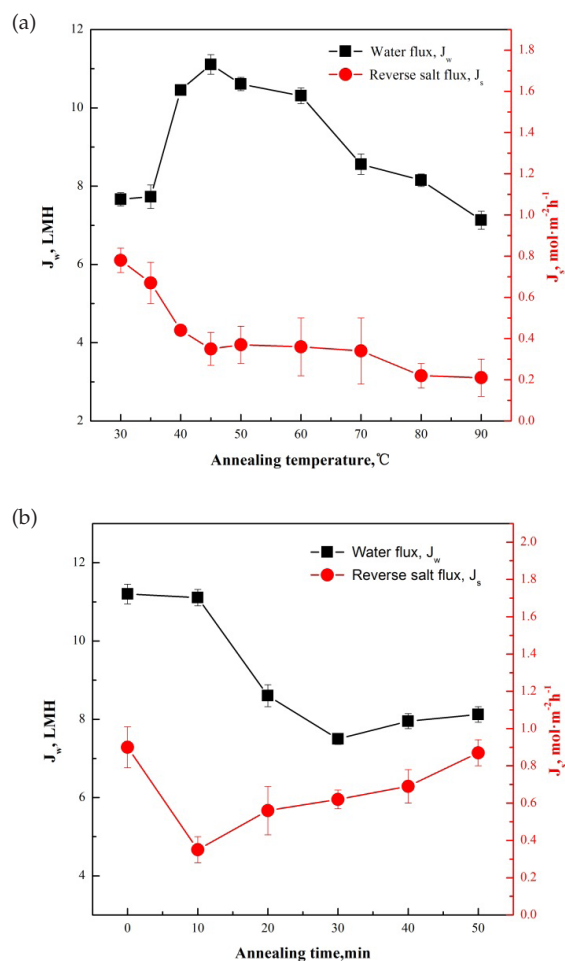


Fig. 8. Effects of annealing temperature and annealing time on membrane performance: (a) annealing temperature (membrane was annealed for 10 min), (b) annealing time (annealing temperature was 45°C).

the annealing time increased from 10–30 min; therefore, membrane pores were large enough to allow more salt molecules to pass through, and the J_s increased. Meanwhile, thermal energy slightly shrank the membrane pore size, reducing the amount of water through the membrane at each interval. Annealing times that exceeded 30 min provided slight assistance in improving the membrane structure; the excessive annealing time even damaged the inner structure of the membrane and led to poor performance.

The performance of the optimal lab made membrane was compared with the commercial HTI membrane at different DS concentration (Table 6). HTI membrane showed good water flux but high reverse salt flux, while the optimal membrane in this work showed better salt rejection performance and reasonable water permeation. The ratio of reverse salt flux to water flux (J_s/J_w) reflected salt selectivity. Membrane with small value of J_s/J_w possessed good performance. The J_s/J_w value of optimal lab made membrane was smaller than HTI membrane, which implied its better selectivity. According to the calculation, the support layer structural parameter, S , of this FO membrane is 651 μm .

Table 6
Performance comparison of commercial HTI membrane and optimal lab made membrane

Membrane ^a	DS concentration (M)	Osmotic pressure	J_w (LMH)	J_s (mol·m ⁻² ·h ⁻¹)	J_s/J_w (M)
HTI membrane	1	47.0	10.1	0.53	0.053
	2	106.6	15.0	0.66	0.044
Lab made membrane	1	47.0	6.7	0.16	0.024
	2	106.6	11.1	0.33	0.030

^amembranes were tested in FO mode(active layers faced the feed solution).

4. Conclusions

In summary, different asymmetric flat-sheet FO membranes with various PET support fabric were obtained by the phase inversion method. The detail influences of casting compositions and preparation conditions on membrane performance were investigated. The major contribution of this investigation can be concluded as below:

- (1) The results of dual solvents showed that the optimal ratio of 1,4-dioxane/acetone is 6. In addition, dual additive systems including PVP and lactic acid have great influence on J_w and J_s . And their concentrations should be control in reasonable range.
- (2) The thickness and pore size of PET support fabric had combined effects on membrane structure and performance. Membranes based on larger pores support fabrics were smoother as well as high water flux and lower reverse salt flux.
- (3) Appropriate evaporation time offered enough time for solvent evaporation and it plays an important role on the membrane performance control. Generally, increase devaporation time will lead to the decrease of water flux and. reverse salt flux. Environmental humidity and the time and temperature of annealing treatment can also influence the membrane performance in some degree.
- (4) The optimized membrane was tested with 2 MNaCl as DS and DI water as FS in FO mode, which exhibited a 11.1 LMH water flux and 0.33 mol·m⁻²·h⁻¹ reverse salt flux. The optimal lab made membrane performed lower salt leakage and better membrane selectivity than commercial HTI membrane.

PVP	—	Polyvinylpyrrolidone
FS	—	Feed solution
DS	—	Draw solution
ICP	—	Internal concentration polarization
PET	—	Polyester
J_w	—	Water flux (L·m ⁻² ·h ⁻¹ , LMH)
J_s	—	Reverse salt flux (mol·m ⁻² ·h ⁻¹)
Δ	—	Solubility parameter
δ_{mix}	—	Solubility parameter of mixed solvent
δ_D	—	Dispersive solubility parameters
δ_P	—	Polar solubility parameters
δ_H	—	Hydrogen-bonding solubility parameters
x_{molar}	—	Volume concentration of component
ρ_w	—	Water density (g·cm ⁻³)
a	—	Membrane effective area (cm ²)
ε	—	Thickness of the wet membrane (cm)
A	—	Water permeability coefficient of the membrane active layer (m·h ⁻¹ ·atm ⁻¹)
B	—	Salt permeability coefficient of the membrane active layer (m/h)
K	—	Resistance to solute diffusion in the membrane support layer (s/m)
D_s	—	Effective solute diffusion coefficient in the membrane support layer (m ² ·s ⁻¹)
S	—	The support layer structural parameter of the membrane (μm)
P1-5	—	Support fabrics with different thickness and pore sizes
M1-5 FO	—	Membrane prepared by optimized dope solution casting on PET support fabric with different thickness and pore sizes.
TFC	—	Thin film composite
P	—	Supolysulf one
MPD	—	m-phenylenediamine

Acknowledgments

This research was financially supported by the National Natural Science Foundation of China (No. 51625804, 51778448) and the Major Science and Technology Program for Water Pollution Control and Treatment (2015ZX07402003-5) of China. We also appreciate the support from the Shanghai Rising-Star Program (No. 17QC1400400).

Nomenclature

CTA	—	Cellulose triacetate
CA	—	Cellulose acetate

References

- [1] T.S. Chung, S. Zhang, K.Y. Wang, J.C. Su, M.M. Ling, Forward osmosis processes: Yesterday, today and tomorrow, *Desalination*, 287 (2012) 78–81.
- [2] E.R. Cornelissen, D. Harmsen, K.F. de Korte, C.J. Ruiken, J.J. Qin, H. Oo, L.P. Wessels, Membrane fouling and process performance of forward osmosis membranes on activated sludge, *J. Membr. Sci.*, 319 (2008) 158–168.
- [3] S. Lee, C. Boo, M. Elimelech, S. Hong, Comparison of fouling behavior in forward osmosis (FO) and reverse osmosis (RO), *J. Membr. Sci.*, 365 (2010) 34–39.
- [4] T.Y. Cath, A.E. Childress, M. Elimelech, Forward osmosis: principles, applications, and recent developments, *J. Membr. Sci.*, 281 (2006) 70–87.

- [5] S. Zhao, L. Zou, C.Y. Tang, D. Mulcahy, Recent developments in forward osmosis: opportunities and challenges, *J. Membr. Sci.*, 396 (2012) 1–21.
- [6] A. Deshmukh, N.Y. Yip, S. Lin, M. Elimelech, Desalination by forward osmosis: Identifying performance limiting parameters through module-scale modeling, *J. Membr. Sci.*, 491 (2015) 159–167.
- [7] D.L. Shaffer, J.R. Werber, H. Jaramillo, S. Lin, M. Elimelech, Forward osmosis: Where are we now?, *Desalination*, 356 (2015) 271–284.
- [8] B.D. Coday, N. Almaraz, T.Y. Cath, Forward osmosis desalination of oil and gas wastewater: Impacts of membrane selection and operating conditions on process performance, *J. Membr. Sci.*, 488 (2015) 40–55.
- [9] R.V. Linares, Z. Li, S. Sarp, S.S. Bucs, G. Amy, J. Vrouwenfelder, Forward osmosis niches in seawater desalination and wastewater reuse, *Water Res.*, 66 (2014) 122–139.
- [10] A. Achilli, T.Y. Cath, E.A. Marchand, A.E. Childress, The forward osmosis membrane bioreactor: a low fouling alternative to MBR processes, *Desalination*, 239 (2009) 10–21.
- [11] R.W. Holloway, A.E. Childress, K.E. Dennett, T.Y. Cath, Forward osmosis for concentration of anaerobic digester centrate, *Water Res.*, 41 (2007) 4005–4014.
- [12] A. Altaee, G. Zaragoza, A. Sharif, Pressure retarded osmosis for power generation and seawater desalination: performance analysis, *Desalination*, 344 (2014) 108–115.
- [13] A. Achilli, T.Y. Cath, A.E. Childress, Power generation with pressure retarded osmosis: An experimental and theoretical investigation, *J. Membr. Sci.*, 343 (2009) 42–52.
- [14] Q. Yang, K.Y. Wang, T.-S. Chung, A novel dual-layer forward osmosis membrane for protein enrichment and concentration, *Separ. Purif. Technol.*, 69 (2009) 269–274.
- [15] E.M. Garcia-Castello, J.R. McCutcheon, M. Elimelech, Performance evaluation of sucrose concentration using forward osmosis, *J. Membr. Sci.*, 338 (2009) 61–66.
- [16] S. Zhang, K.Y. Wang, T.-S. Chung, Y. Jean, H. Chen, Molecular design of the cellulose ester-based forward osmosis membranes for desalination, *Chem. Eng. Sci.*, 66 (2011) 2008–2018.
- [17] L. Huang, J.R. McCutcheon, Impact of support layer pore size on performance of thin film composite membranes for forward osmosis, *J. Membr. Sci.*, 483 (2015) 25–33.
- [18] S. Zhang, K.Y. Wang, T.-S. Chung, H. Chen, Y. Jean, G. Amy, Well-constructed cellulose acetate membranes for forward osmosis: minimized internal concentration polarization with an ultra-thin selective layer, *J. Membr. Sci.*, 360 (2010) 522–535.
- [19] C. Tsay, A. McHugh, Mass transfer modeling of asymmetric membrane formation by phase inversion, *J. Polym. Sci. Part B: Polymer Physics*, 28 (1990) 1327–1365.
- [20] J. Wijmans, J. Baaij, C. Smolders, The mechanism of formation of microporous or skinned membranes produced by immersion precipitation, *J. Membr. Sci.*, 14 (1983) 263–274.
- [21] R. Pilon, B. Kunst, S. Sourirajan, Studies on the development of improved reverse osmosis membranes from cellulose acetate–acetone–formamide casting solutions, *J. Appl. Polym. Sci.*, 15 (1971) 1317–1334.
- [22] T.P.N. Nguyen, E.-T. Yun, I.-C. Kim, Y.-N. Kwon, Preparation of cellulose triacetate/cellulose acetate (CTA/CA)-based membranes for forward osmosis, *J. Membr. Sci.*, 433 (2013) 49–59.
- [23] B. Mi, M. Elimelech, Gypsum scaling and cleaning in forward osmosis: measurements and mechanisms, *Environ. Sci. Technol.*, 44 (2010) 2022–2028.
- [24] W.A. Phillip, J.S. Yong, M. Elimelech, Reverse draw solute permeation in forward osmosis: modeling and experiments, *Environ. Sci. Technol.*, 44 (2010) 5170–5176.
- [25] A. Tiraferri, N.Y. Yip, A.P. Straub, S.R.V. Castrillon, M. Elimelech, A method for the simultaneous determination of transport and structural parameters of forward osmosis membranes, *J. Membr. Sci.*, 444 (2013) 523–538.
- [26] A. Tiraferri, N.Y. Yip, W.A. Phillip, J.D. Schiffman, M. Elimelech, Relating performance of thin-film composite forward osmosis membranes to support layer formation and structure, *J. Membr. Sci.*, 367 (2011) 340–352.
- [27] X. Liu, H.Y. Ng, Double-blade casting technique for optimizing substrate membrane in thin-film composite forward osmosis membrane fabrication, *J. Membr. Sci.*, 469 (2014) 112–126.
- [28] K.Y. Wang, R.C. Ong, T.-S. Chung, Double-skinned forward osmosis membranes for reducing internal concentration polarization within the porous sublayer, *Indust. Eng. Chem. Res.*, 49 (2010) 4824–4831.
- [29] M. Yasukawa, S. Mishima, M. Shibuya, D. Saeki, T. Takahashi, T. Miyoshi, H. Matsuyama, Preparation of a forward osmosis membrane using a highly porous poly ketone micro filtration membrane as a novel support, *J. Membr. Sci.*, 487 (2015) 51–59.
- [30] X. Lu, L.H. Arias Chavez, S. Romero-Vargas Castrillon, J. Ma, M. Elimelech, Influence of active layer and support layer surface structures on organic fouling propensity of thin-film composite forward osmosis membranes, *Environ. Sci. Technol.*, 49 (2015) 1436–1444.
- [31] M. Sairam, E. Sereewatthanawut, K. Li, A. Bismarck, A. Livingston, Method for the preparation of cellulose acetate flat sheet composite membranes for forward osmosis—desalination using MgSO_4 draw solution, *Desalination*, 273 (2011) 299–307.
- [32] B. Kunst, P. Goran, On the pore size distribution in asymmetric reverse osmosis membranes, *J. Colloid Interface Sci.*, 87 (1982) 575–576.